Experimental investigation of a novel vertical loop-heat-pipe PV/T heat and power system under different height differences

Min YU[a,b,c], Fucheng Chen[d], Jinzhi ZHOU[b,c] , Yanping Yuan[b], Yi FAN[c], Guiqiang LI[c], Xudong ZHAO [c*], Zhangyuan WANG [d], Jing LI[c], Siming Zheng[d]**

[a] SWJTU-Leeds Joint School, Southwest Jiaotong University, Chengdu, China

[b] School of Mechanical Engineering, Southwest Jiaotong University, Chengdu, China

[c] Research Centre for Sustainable Energy Technologies, University of Hull, United Kingdom

[d] School of Civil and Transportation Engineering, Guangdong University of Technology, China

Abstract: For a novel vertical solar loop-heat-pipe photovoltaic/thermal system, the height difference between evaporator and condenser plays an important role in the heat transport capacity, which has significant impact on the solar thermal efficiency and parametrical optimization of this system. Therefore, based on the results derived from the authors' previous analytical investigation and computer modelling studies, a prototype of this novel system was designed, constructed, and an experimental investigation under different height difference was undertaken to study the impact of height difference on the system performance. It was found that the relationship between the solar thermal efficiency of this vertical system and the height difference is nonlinear. In present study, the optimal height difference is around 1.1m, which was selected as an optimal value for the following experimental investigations, and below 1.1m, the PV module surface temperature decreased with the increase of the height difference. Furthermore, the transient solar thermal and electrical performance of this system with

* Corresponding authors.
Email address: Xudong.Zhao@hull.ac.uk (Xudong ZHAO); zwang@gdut.edu.cn (Zhangyuan WANG)

the selected optimal height difference was investigated under outdoor real weather condition. These results of this experimentation can help optimize the system construction and thus help to develop the high thermal performance and low-cost solar PV/T system for space heating and power generation.

Keywords: Micro-channel; Loop heat pipe; PV/T; Height difference; Efficiency

Nomenclature

Parameters

A	Area, m^2
c	Specific heat, kJ/(kg*K)
m	Mass, kg
F	Efficiency factor
G	Solar radiation, W/m^2
H	Height difference (HD), m
I	Current, A
MCT	Micro-channel Tube
P	Output power, W
q	Heat output, W
R	Thermal resistance ,W/K
Re	Reynolds number
RE	The relative error
RME	The experimental relative mean error
T	Temperature, ℃
u	Velocity, m/s
U	Output voltage, V

x_i	Variable (i=1, 2 … n)
y	A given dependent variable

Greek letters

β	Temperature coefficient
η	Efficiency
η_{rc}	Initial electrical efficiency at reference temperature
μ	dynamic viscosity ,Pa·s

Subscripts

e	Electrical
in	Inlet
o	Overall
out	Outlet
PV	Photovoltaic
PVT	Photovoltaic/thermal
rc	Reference condition
th	Thermal
w	Water

1. Introduction

It is reported by the International Energy Agency (IEA) that during 2017-2023, renewables will meet more than 70% of global electricity generation growth. The growth of the solar photovoltaic (PV) is larger than all other renewables in combination, while China remains the absolute solar PV leader by far, holding almost 40% of global installed PV capacity in 2023[1]. However, it has been proved that the increment by 1℃ of the PV cells' temperature would result in around 0.25% to 0.5% linear drop of the solar electrical efficiency [2][3] , which is in the range of 4%-20%[4] . In order to control the PV cells' temperature, methods were utilized to take away the accumulated heat of the solar PV modules and then to make full use of the removed heat, which is known as solar photovoltaic/thermal (PV/T) technology[5], making advanced utilisation of absorbed solar energy as both electricity and heat by one module. According to different heat transfer mediums, the PV/T systems can be divided into air-based PV/T systems [6][7] where the PV cells were cooled by naturally or mechanically ventilated air; water-based PV/T systems [8][9] cooled by circulating water across the back-side coils or tubes; and heat pipe / loop heat pipe-based PV/T systems cooled by applying (loop) heat pipe through the working fluid evaporation and condensation to achieve heat removal and recovery of the PV/T system [10].

During recent decades, the application of Loop Heat Pipe (LHP)/Heat Pipe (HP) for PV/T systems has obtained wide attention owing to its high heat transfer capability, no working fluid leakage risk, and no frozen problems in winter. Zhang et al. [11] introduced a novel solar photovoltaic/loop-heat-pipe (PV/LHP) heat pump system for hot water generation, and experimentally investigated the performance of the system, indicating that the electrical, thermal and overall efficiency of the PV/LHP module were around 10%, 40% and 50% respectively under the given experimental conditions. Zhang et al.[12]also investigated the dynamic performance of the novel PV/LHP heat pump system for potential use in space heating or hot water generation, applying theoretical computer simulation and experimental validation to analyse and make comparison. He et al. [13] proposed the novel heat pump assisted solar façade loop-heat-pipe water heating system and studied its operational performance by applying both theoretical and experimental methods, indicating that the average thermal efficiency of the LHP module was around 71% with the heat pump's assistance.

However, almost all existing loop heat pipes integrated into the PV/T system were designed and constructed with round tubes and plate fins (RTPF) with linear contact area in touching on the PV model. This results in relative higher heat transfer resistance. Therefore, micro channel loop heat pipe (MCLHP) applying flat Al-flat tube, which can touch well with the PV panel with surface contact is utilized. This MCLHP is one kind of two phase (evaporation/condensation) loop heat pipe heat transport device, comprising the micro-channel array integrated evaporator, condenser, separate vapour and liquid transportation lines, and compensation chamber[14], was recently applied to cool PV cells and make use of the solar thermal energy [15][16].This kind of micro-channel loop heat pipe can greatly enhance the heat transfer ability with smaller cross-section area, consume no power for refrigerant compressors through longer distance, and has more compact structure compared to heat pipe with round tubes and plate fins[17] . Furthermore, owing to its flat-plate surface, the micro-channel array has an advantage of easy binding with the PV model. Within these limited researches/studies, the authors have previously [15][16][18] developed the novel solar micro-channel loop heat pipe PV/T system filled with refrigerant R134a, which has been investigated through computer modelling and theoretical analysis from different perspectives. Both the separate multiple-micro-channel evaporator and the condenser of this LHP-PV/T system are laid vertically, which make the refrigerant gravity inside the loop to be the driving force to the downward fluid flow. In that case, a higher HD will cause bigger thermal resistance, while a lower HD could result in lower gravity. The height difference between the evaporator and the condenser will therefore play an important role in the performance of this system. Zhao et al. [19] designed and theoretically studied a novel LHP solar heating system, indicating that variation in the height difference between the evaporator and the condenser would cause different system performance. In regards with the LHP solar system and the weather condition in Beijing, they found when height difference is larger than 0.4m, the system would have enough heat transfer capacity for the absorbed heat. At an early stage, Zhang et al. [20]design a LHP based solar thermal façade heat pump system mentioning that HD results in the gravity effect to control the liquid feeding speed and thus to balance the liquid evaporation and delivery. At the same time, they [21] also investigated a solar photovoltaic/loop-heat-pipe (PV/LHP) heat pump system with different height difference from the evaporator to the condenser and found that the capillary limit, governing the heat transfer capacity when the heat difference was lower than 1.1m, raised with the height difference, and a linear relationship between the height difference and the capillary limit was also proved to be existing because of the effect of gravity, which is directly influenced by height difference. However, some researchers ignored the impact of height difference and supposed that assuming the evaporator outlet temperature equals to the condenser inlet temperature is enough[22][23].

In terms of this key point, this paper experimentally investigated the impact of the height difference between the evaporator and the condenser on the solar thermal performance of this novel vertical LHP-PV/T system, aiming at finding an optimal value of the height difference to optimize the system construction and thus helping to develop an impact, easy installed, high thermal performance and low-cost solar PV/T system for space heating and power generation.

2. Description of this novel vertical LHP-PV/T system

Based on the results derived from the analytical investigation and computation studies presented in the authors' previous papers[15][16], this novel vertical LHP-PV/T system was designed as schematically shown in **Figure 1**. This system comprises: (1) multiple micro-channel array integrated into PV/evaporator; (2) co-axial triple-pipe heat exchanger applying PCM to be the condenser; (3) separate vapour and liquid transportation lines; (4) PV module covered with glass without air gap, which is pressed on the aluminium (Al) plate, and as a result, reducing the thermal resistance between the PV cells and the Al plate compared with the conventional PV panel with thermal grease. Meanwhile, this novel system has three crucial innovations: (1) The upper liquid feeding pipe working as the chamber of a LHP and also in parallel, a vapour collecting pipe integrated on the top of the micro-channel evaporator, which can effectively gather the vapour from the micro-channels as shown in **Figure 1(a)**, and importantly, can separate the vapour and liquid to reduce the resistance from the rising vapour to the falling liquid; (2) Inside the upper liquid feeding tube, four tiny holes are opened on the side wall of each micro-channel as shown in **Figure 1(c)(d)**, which can distribute the condensing liquid across the inner micro-channel walls and achieve continuous liquid film on the rough/wicked side walls of micro-channels, thus improving the heat transfer ability which has been validated by the investigation on heat transfer limits; (3) Triple-pipe heat exchanger with Phase Change Materials (PCM) as shown in **Figure 1(b)**, which is designed to condense the evaporated fluid coming from the micro-channel evaporator and store the excess heat by melting the PCM inside the outer tube.

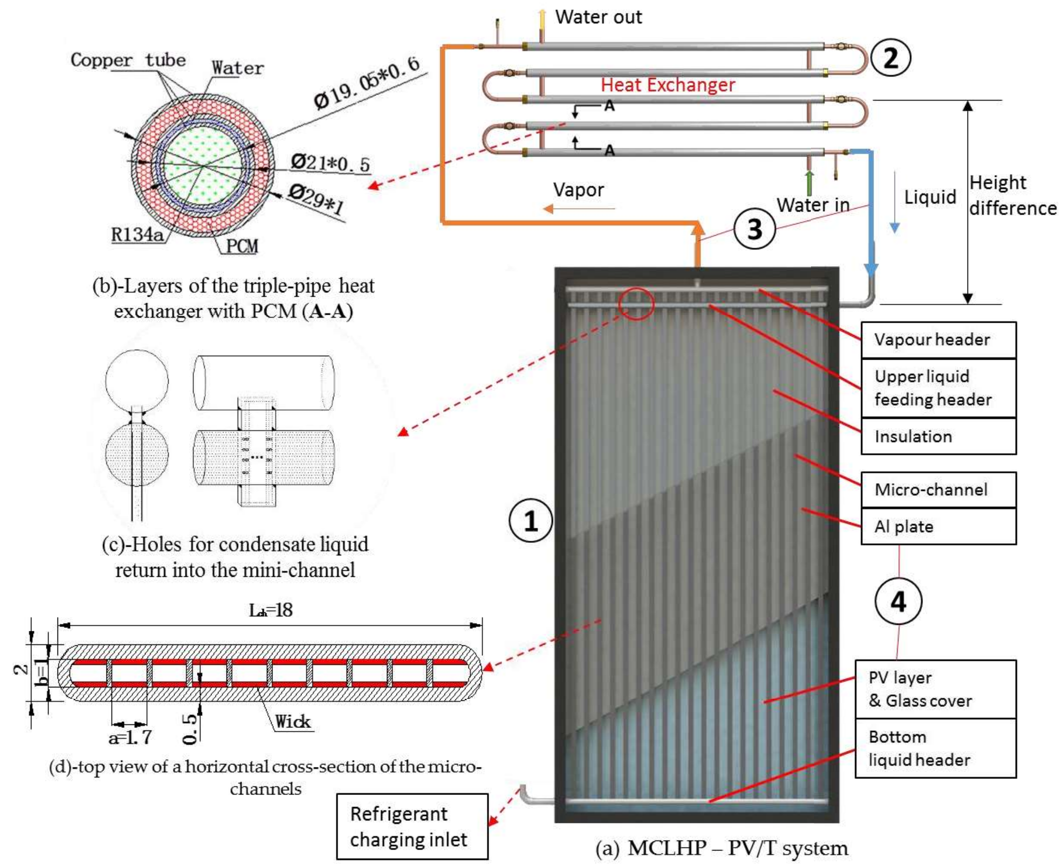

Figure 1. The novel solar LHP-PV/T heating and power system

When the PV/evaporator receives the solar radiation striking on its upper surface, most of the solar radiation is absorbed by the PV/T panel, part of which is converted into electricity by PV cells to supply power and the rest is finally transformed into thermal energy. The thermal energy is absorbed by the Al plate and then transferred to the micro-channels, thus evaporating the working fluid (Refrigerant R-134a) inside the channels. The evaporated fluid floating from the micro-channel array is collected in the upper vapour header and then transported towards into the heat exchanger (condenser) through the single vapour transportation line. In the heat exchanger, the latent heat from the vapour condensing in the central pipe is transferred to the water flowing inside the middle annulus tube, then the hot water will be circulated for space heating etc. At the same time, the heated water conducts the melting of the PCM inside the outer annulus tube to storage excess thermal energy and also to keep the water temperature within a certain temperature range. As a result, the condensed fluid from heat exchanger, driven by gravity, flows directly into the upper liquid feeding header through the single liquid transportation line, and then penetrates the micro-channel wall via the tiny holes to formulate the continuous downward liquid streams (films) among the porous wick to keep the side wall of channels at the wet condition, which can thus offer timely replenishment of the evaporating fluid for absorbing heat from the solar energy. All these processes formulate the cycle loop as illustrated in **Figure 2.**

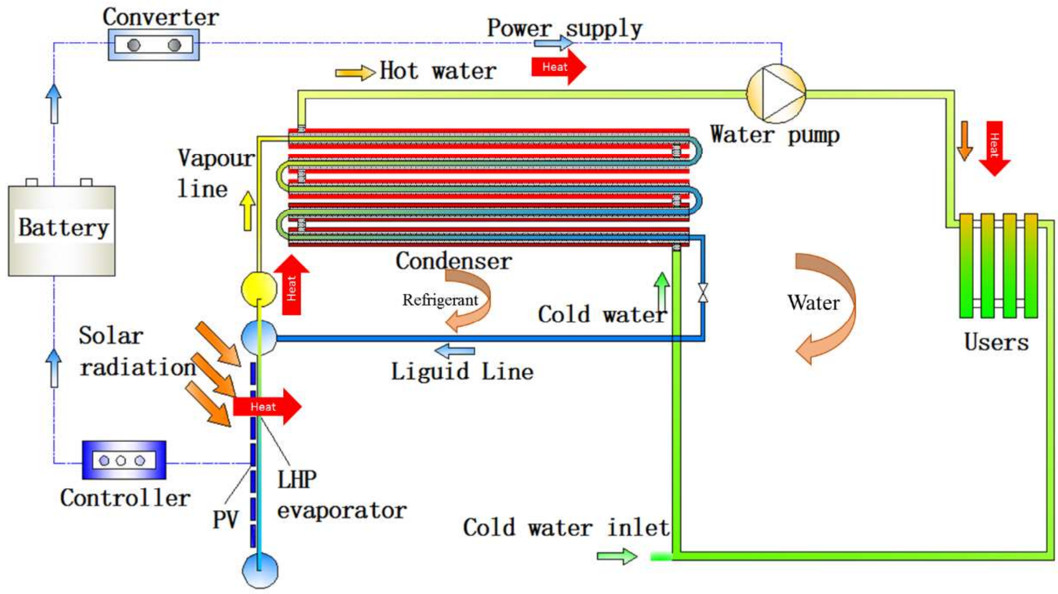

Figure 2. Cycle loop of the novel solar LHP-PV/T heating system

2. Experimental setup and procedure

3.1 Experimental set up

The integrated prototype of this vertical LHP-PV/T heating and power system was built in an indoor space (Lab. in Guangdong University of Technology, China) as presented in **Figure 3**, and equipped with various measurement instruments and sensors, including pyranometer, rotameter, thermocouples/temperature probes, and pressure sensors, which were installed at appropriate positions to measure solar radiation, flow rate, temperature and pressure, respectively. In addition, the Solar Power Controller (MPPT) was used to be both the electrical recorder and converter. All the testing outputs were transmitted into relevant data logger and temperature recorder, respectively, and then gathered to the computer. The parametrical specifications of this system are listed in **Table 1.**

Table 1. Parametrical specifications of the vertical LHP-PV/T system

Parameters	**Value**
Micro-channel port width	0.0017 m
Micro-channel port height	0.001m
Evaporator length	1.9 m
Number of micro-channel flat heat pipes	20
Number of micro-channel ports	10
Operating temperature range	20-60 ºC
Transportation line outer diameter	0.0174 m
Transportation line inner diameter	0.015 m
Liquid head length	1m
Liquid Head diameter	0.022 m
Vapour header length	1m
Hole diameter	0.00075 m
Transportation line length	1.5/1.5 m
Heat exchanger central tube total length	5 m
Heat exchanger central tube diameters	0.016/ 0.017 m
Heat exchanger middle tube diameters	0.019/ 0.021 m
PCM tube diameters	0.027/ 0.029 m
PCM melting temperature	44 ºC
PCM density	800 kg/m^3
PCM Latent Heat	242 kJ/kg
PCM thermal conductivity	0.18 W/(m·K)
PCM Maximum operating temperature	300 ºC

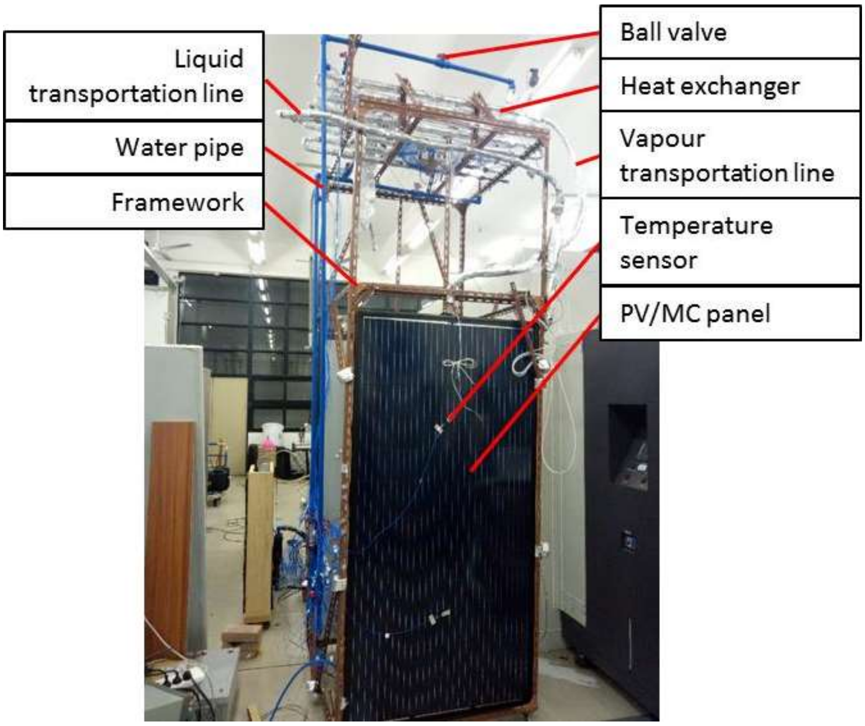

Figure 3. Construction of the novel solar LHP-PV/T heating system

3.2 Experimental process

In order to study the impact of height difference between the PV/evaporator and the condenser on the performance of this novel solar LHP-PV/T system, based on the authors' previous analytical computation investigation of heat transfer limits under different height differences[15], which illustrated that from 0.1m to 1m, a larger height difference between the evaporator and the condenser leads to a higher capillary limit and thus a higher heat transfer capacity. It is found that the heat transfer limit of HD at 1.0m is larger than that of 0.6, the difference between 0.6 and 1.0 is larger than that between 0.3 and 0.6, therefore, for present experimental study, 0.7 is set as start-up, and four different height difference (i.e. 0.7 m, 0.9 m, 1.1 m, 1.3 m with an increment of 0.2 m) were carried out under relatively steady conditions to determine the optimal value. The measurement positions are presented in **Figure 4**, where the average solar radiation is maintained as 565±10 W and the ambient temperature is around 30 ℃. The steady state defined in this experiment is that the thermal properties of the MCLHP stay the same against the operating time under dedicated testing mode.

Each lab test started at 15:30 pm and run for sufficient hours to obtain the relative steady state data. After the optimal height difference confirmed, this experimental system was moved to outdoor to test under the real weather from 9:30 am to 16:30 pm. During all the tests, the measurement data was recorded at 30s interval and logged into the computer to enable the follow-on analysis to be completed.

The analyses of the experimental data need to consider that the potential equipment uncertainties, e.g., the tolerance of the solar radiation (±10W) and the temperature measurement discrepancy (±0.1℃). Additionally, there are some potential random errors, which may be caused by personal fluctuation, random electronic data logger fluctuation and influences of friction inside cooling pipes due to impure cooling water, etc.

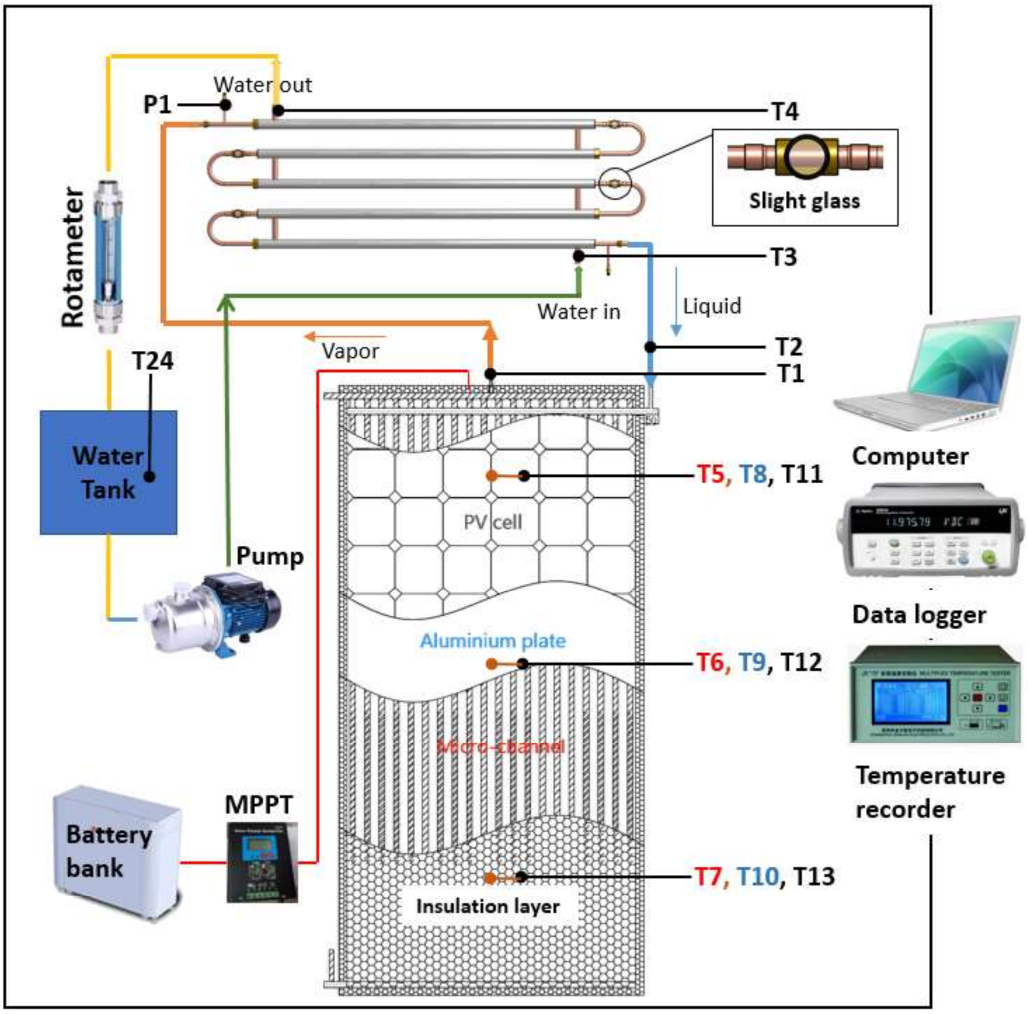

P1 - Pressure of the LHP; **T5, T6, T7** - Surface temperature of PV panel; **T8, T9, T10** - Surface temperature of Al plate; **T11, T12, T13** -Temperature of micro-channel array

Figure 4. Experimental setup

3.3 Error analysis

Based on the error propagation theory, the experimental error of the independent variables, such as temperature, output power and solar radiation, is determined by the accuracy of the specific measurement instrument; while the error of dependent variables, such as solar thermal and electrical efficiencies, can be calculated based on the error of the independent variables. Thus, for a given dependent variable y:

$$y = f(x_1, x_2, \cdots, x_n) \tag{1}$$

The relative error (RE) can be calculated by [24][25]:

$$RE = \frac{dy}{y} = \frac{\partial f}{\partial x_1}\frac{dx_1}{y} + \frac{\partial f}{\partial x_2}\frac{dx_2}{y} + \cdots + \frac{\partial f}{\partial x_n}\frac{dx_n}{y} \quad , \tag{2}$$

where x_i $(i = 1,2, \ldots, n)$ is the variable of the dependent variable y; and $\partial f/\partial x_i$ is the error transfer coefficient of the variables.

The experimental relative mean error (RME) during the test period can be expressed as:

$$RME = \frac{\sum_1^N |RE|}{N} \tag{3}$$

Based on the Eqs. (1) to (3), the REMs of all the variables were calculated and the results were listed in **Table 2.** All the experimental relative mean errors are in the acceptable range.

Table 2. The experimental RMEs of the variables

Variable	T (%)	G (%)	η_e (%)	η_{th} (%)
RME	0.067	2.0	4.2	21.4

4 Theoretical equations

4.1 Thermal resistance

Based on the theoretical model established by the authors in previous works [26,27], it is assumed that there would be no existing temperature gradient along the length direction of the Micro-channel heat pipe evaporation section, owing to the even heat input. Then the total useful solar heat transferred into the water in the middle annulus tube of the co-axil triple-tube heat exchanger from absorbed Al plate can be calculated according to the Hottel-Whillier model[26][28][29]:

$$Q_u = LWF_{th}[q_{abs} - K_L(T_w - T_a) - q_e] \tag{4}$$

Where, L and W are the length and width of the Al plate (m); q_{abs} is the absorbed heat per unit (W/m^2); q_e is the solar energy converted into electricity; T_w is the mean temperature of water in the middle annulus tube of the co-axil triple-pipe heat exchanger; F_{th} the thermal efficiency factor of the PV/T system which, representing the ratio of the actual useful heat gain by the system to the overall converted solar heat at a certain working fluid temperature, can be expressed as:

$$F_{th} = \frac{K_L^{-1}}{\frac{LW}{N_{MCT}}\left\{\frac{1}{LK_L\left[\left(\frac{W}{N_{MCT}} - D_{MCT}\right)F_f + \frac{D_{MCT}}{1 + r_{p-Al}K_L}\right]} + \sum_{i=1}^{6} R_i\right\}} \tag{5}$$

Where, N_{MCT} is the number of the micro-channel flat tube; $\sum R_i$ is the overall thermal resistance of from the absorbed Al plate to the working fluid.

This thermal efficiency factor of this system which, is a constant figure under the fixed physical and operating condition, takes consideration of all the thermal resistances from the absorbed Al plate to the water in the middle annulus tube of the co-axil triple-pipe heat exchanger, including: (1) thermal resistances between the PV cells and absorbed Al plate ($R_1 = R_{p-Al}$); (2) thermal resistance of the micro-channel heat pipe wall ($R_2 = R_{MC}$); (3) equivalent radial thermal resistance of the flow ($R_3 = R_{eq,f}$), which is composed of the resistance of the liquid film from holes on the side of the channel $R_{lf,c}$ assumed parallel to the radial thermal resistance of the two phase flow on the other side of the channel $R_{eq,v}$; (4) the resistance of the axial vapour flow ($R_4 = R_{v,a}$); (5) the resistance of the condensation two phase flow ($R_5 = R_{tp,c}$); (6) the thermal resistance of the central tube wall of the co-axial triple-pipe heat exchanger ($R_6 = R_{HE1}$). These resistances will be analysed in the following sections. And before analysing, it should be noticed that the resistance of the silicon sealant and the heat capacity of the adhesive layer are neglected, resulting from their significantly smaller values compared to other factors [22].

Among these thermal resistances, the equivalent radial thermal resistance of the flow is composed of the resistance of the liquid film from the holes on one side of the micro-channel wall, which is closely related to the height difference between the evaporator and the condenser, and the resistance of the two-phase flow flowing along the other two sides of the channel port, where these two type of thermal resistance are assumed to be parallel. Thus the equivalent radial thermal resistance of the flow can be expressed as:

$$R_{eq,f} = \left(\frac{1}{R_{lf}} + \frac{1}{R_{tp,f}}\right) \tag{6}$$

Where, R_{lf} is the total thermal resistance of the condensate liquid film with thickness of δ_{lf} at the two opposite micro-channel walls with holes, which can be calculated by:

$$R_{lf} = \frac{\delta_{lf}}{\lambda_{lf}(2a \times L_{MC})\mathrm{N}_{MCT}N_{ch}} \tag{7}$$

And $R_{tp,f}$ is the thermal resistance of the two-phase flow flowing on the other two sides wall of the micro-channel expressed as:

$$R_{tp,f} = \frac{1}{2b\varepsilon_{of}L_{MC}h_{tp}\mathrm{N}_{MCT}N_{ch}} \tag{8}$$

Where, h_{tp} calculated by considering the overall fin efficiency ε_{of} in the micro-channel heat pipe is the overall heat transfer coefficient of the two-phase flow in the micro-channel. The h_{tp} and ε_{of} can be obtained from the authors' previous paper[26]. δ_{lf} is the liquid film thickness which, assumed the same along the adjacent wall, is linked to the pressure difference between the outlets of the evaporator and condenser, where the height difference is denoted by H_{ce}. Based on this height difference, the condensed liquid penetrate the tiny holes on the side wall of the micro-channels to formulate this liquid film, which can be approximated as

$$\text{When } Re \leq 400, \quad \delta_{lf} = \left(\frac{3\mu_l^2}{\rho_1^2 g}\right)^{1/3} Re^{1/3} \ ;$$

$$\text{When } Re > 400, \quad \delta_{lf} = 0.369\left(\frac{3\mu_l^2}{\rho_l^2 g}\right)^{1/2} Re^{1/2}$$

Where μ_l is the liquid dynamic viscosity ($Pa \cdot s$);ρ_l is the liquid density (kg/m^3); Re is the Reynolds number given by

$$Re = \frac{\rho u_{lf}}{\mu_1}\delta_{lf} \tag{9}$$

u_{lf} is the superficial velocity of the liquid film flow expressed as following, which depends on the pressure difference of the loop and is assumed to be the same for each tiny hole opened on the side wall of the micro-channel.

$$u_1 = A_h \frac{(2gH_{ev-co})^{1/2}}{A_{lf}(1-C_d^2(d_h/d_{lh}))} \tag{10}$$

Where, A_h is the cross-sectional area of the tiny hole; H_{ev-co} is the height difference between the top of the PV/micro-channel evaporator and the condenser working as the driving pressure head; d_h and d_{lh} are the diameter of the tiny hole and the liquid header respectively; A_{lf} is the liquid film cross-sectional area expressed as:

$$A_{lf} = \delta_{lf} a \tag{11}$$

And C_d is the discharge coefficient of the flow from the upper liquid header to the tiny holes, which can be calculated by [30][31]:

$$C_d = 0.611\left[87\left(\frac{4.5\mu_l}{\rho_l d_h\sqrt{gH_{ev-co}}}\right)^{1.43} + \left(\frac{4.5\mu_l}{\rho_l d_h\sqrt{gH_{ev-co}}}\right)^{-1.26}\right]^{-0.7} \tag{12}$$

4.2 Key indicators

A number of key indicators, including the output power, solar electrical and thermal efficiencies, and overall solar efficiency, were applied to evaluate the performance of the LHP-PV/T system. These are defined as below:

Output power of PV/T (P_{PVT}) can be expressed as:

$$P_{PVT} = U_{PVT} I_{PVT} \ , \tag{13}$$

where, U_{PVT} is the output voltage of the PV/T panel and I_{PVT} is the current of the PV/T panel.

Solar electrical efficiency (η_e) can be expressed as:

$$\eta_e = \frac{P_{PVT}}{G \cdot A_{PV}} = \frac{U_{PVT} I_{PVT}}{G \cdot A_{PV}} \quad , \tag{14}$$

where, η_e is the electrical efficiency of PV/T panel, G is the solar radiation, and A_{PV} is the PV area of base panel. Alternatively, Electrical efficiency (η_e) can be written as:

$$\eta_e = \eta_{rc}[1 - \beta_{PV}(T_{PV} - T_{rc})] \ , \tag{15}$$

where, η_{rc} is the initial electrical efficiency at reference temperature, β_{PV} is temperature coefficient, T_{PV} is PV cells temperature at operation, and T_{rc} is reference temperature.

Solar thermal efficiency (η_{th}) can be expressed as:

$$\eta_{th} = \frac{q_{th}}{G \cdot A_{PV}} = \frac{c_w m_w (T_{wout} - T_{win})}{G \cdot A_{PV}} , \tag{16}$$

where, q_{th} is the useful thermal energy (heat) output of the system (W); c_w is the specific heat at constant pressure of liquid (water, 4186 W/kg/°C), m_w is the mass flow rate of water flow in co-axial triple-pipe heat exchanger (kg/s), T_{wout} and T_{win} is the outlet and inlet water temperature of the triple-pipe heat exchanger (°C).

Overall solar efficiency (η_o) can be expressed as:

$$\eta_o = \eta_e + \eta_{th} \tag{17}$$

5 Results and discussion

5.1 Determination of optimal height difference

Height difference between the PV/evaporator and the condenser in this novel solar LHP-PV/T system plays a significant role. If the height difference is too small, the gravity is not enough to drive the liquid to feed back the micro-channels leading to dry out in the evaporator section, and then the lower section of the micro-channels could have no liquid to saturate the wick, which would result in increasing wall temperature and the solar thermal performance degradation. While if the height difference is too high, the vapour transportation would be too long and the total volume of the loop will significantly increase which means that the loop needs more working fluid filling mass. In addition, higher height difference leads to higher driven force to accelerate the liquid feeding back velocity, which will cause excess liquid and result in the micro-channels full of liquid when bubbles form due to boiling, and finally decrease the evaporation heat transfer ability. Furthermore, too large height difference could consequently enlarge the size of the system thus make it not compact to install and apply. Therefore, an optimal value of height difference of this system exerts a pivotal role to optimize the system size and make sure that the system operates safely and efficiently.

In this process, the PV module surface temperature and solar thermal efficiency were applied to evaluate the performance of this novel solar LHP-PV/T heating system under various height difference. The height difference is defined to be the distance from the refrigerant inlet of the PV/evaporator to the middle position of the condenser as shown in **Figure 1.**

For the given testing condition (i.e. ambient temperature at 30±0.5℃, cooling water flow rate at 0.17, solar radiation at 565±10 W, different inlet water temperature), the solar thermal efficiencies of the system and the outlet water temperature under different height difference were presented in **Figure 5**. It was found that increasing inlet water temperature led to decreasing in solar thermal efficiency of the vertical LHP-PV/T system when keeping the height difference constant. However, for the different inlet water temperature groups, the parabola-like trend of the solar thermal efficiency variation with the different height difference is obvious, where there are maximum thermal efficiencies occurring in the height difference of 1.1m, i.e. the optimization height difference is not at the highest HD of 1.3m in this testing condition, which is a little different from the previous single testing result in reference[26] with larger refrigerate filling ratio. The reason for this may be that (1) when the height difference increased, the thermo-siphon effect caused by the density difference between the refrigerant vapour and liquid was enhanced, leading to the increased heat transfer rate from the evaporator to condenser, thus the heat transfer capacity of the LHP increased. As a result, the solar thermal efficiency of the system was increased firstly; (2) when the height difference is above 1.1m, it is obvious that the solar thermal efficiency start decreasing which may because that higher height difference caused longer vapour/liquid transportation line and the total volume of the loop will significantly increase which means that the loop needs more working fluid filling mass which will be experimentally investigated in next step in details. In addition, height difference of 1.1 m can make the system more compact leading lower cost than that of 1.3 m. Therefore, in present study, the optimal height difference is around 1.1m, and owing to the construction frame and experiment limitations, 1.1m was selected as an optimal value of height difference between evaporator and heat exchanger for the following experimental investigations.

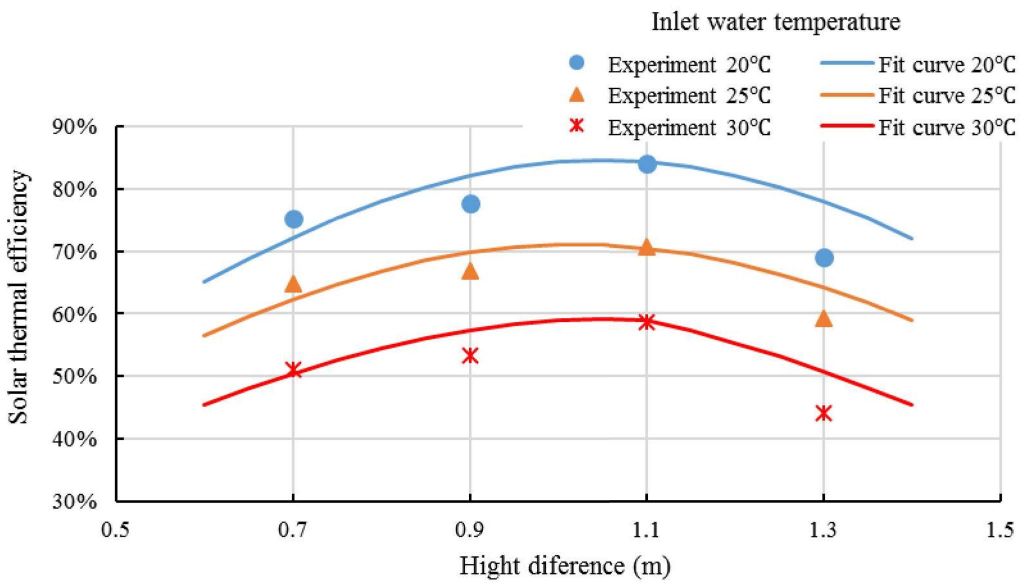

Figure 5. Solar thermal efficiency changing with height difference

The PV module surface temperature against the height difference at the same given testing condition is shown in **Figure 6**. It is found that at the first operation hour, PV module surface temperature shows lowest value at the height difference of 1.1 m, and then PV module surface temperature shows lowest value at the height difference of 1.3 m and that of 1.1 m become the second lowest value. When the system becomes steady, the PV module surface temperature almost decreases with the rise of the height difference. This may be because higher height difference causes larger driven force which is superior to the heat transfer ability to efficiently cool the PV module thus leading lower PV module surface temperature.

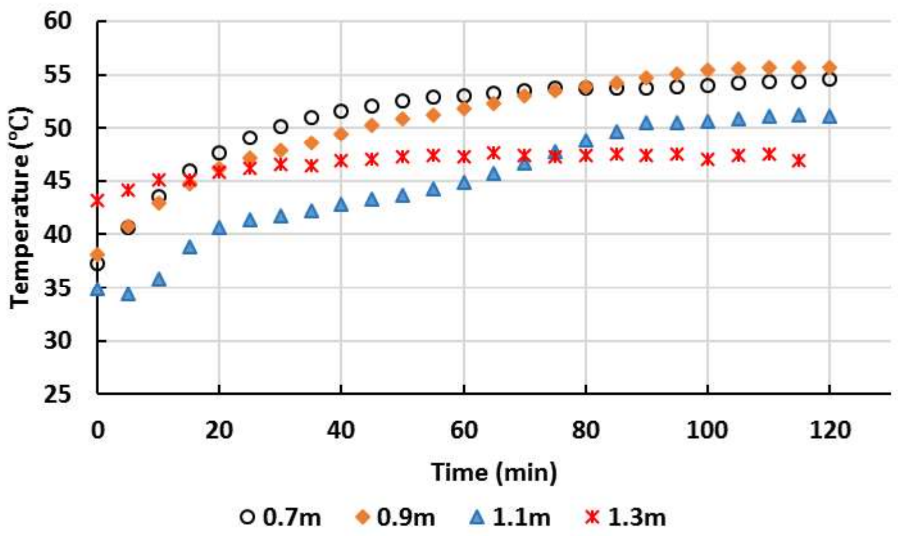

Figure 6. PV module surface temperature against height difference

5.2 Temperature distribution for optimal height difference under steady solar radiation

Keeping the parameters unchanged (i.e., height difference at optimal value of 1.1 m, ambient air temperature at 30±0.3ºC, initial inlet cooling water temperature at 19±1 ºC, cooling water flow rate at 0.17 m^3/h), the temperature distribution of different components of the PV/evaporator was experimentally investigated. **Figure 7** shows the variation of the PV/T evaporator components surface temperature against operation time. It is found that (1) there is a start-up process at the test beginning, when the temperature of different components is rising with operating time, and then becomes steady state; (2) the highest temperature of the PV model surface is still lower than 55 ºC, which is lower than existing PV/T system at the same solar radiation condition, indicating that the micro-channel loop heat pipe shows an efficient heat transfer ability to cool the PV model; and (3) the mid-level of panel has higher temperature than the lower and higher levels of the panel, indicating that the simulated solar radiation distribution across the panel is non-uniform and mid-level of the panel receives higher radiation compared to the lower and upper parts.

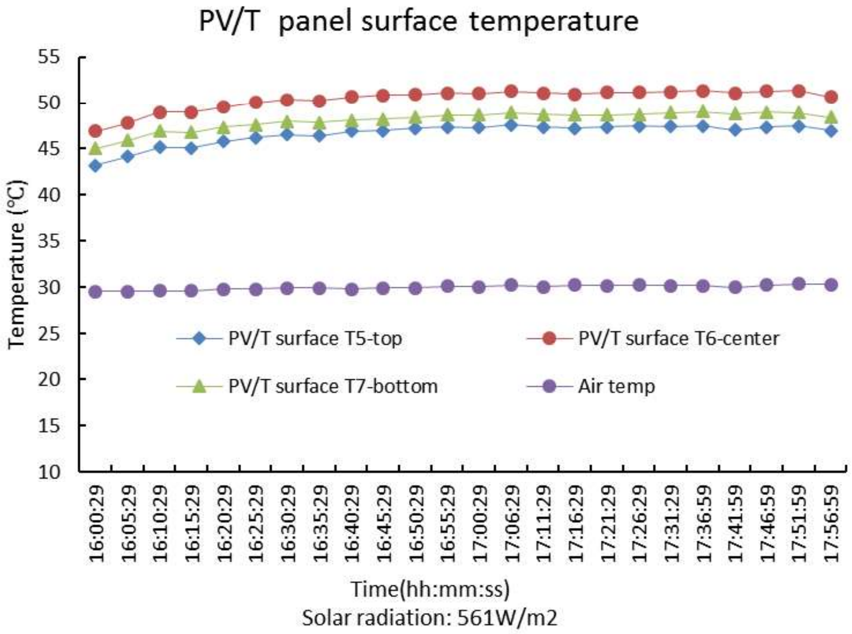

(a)

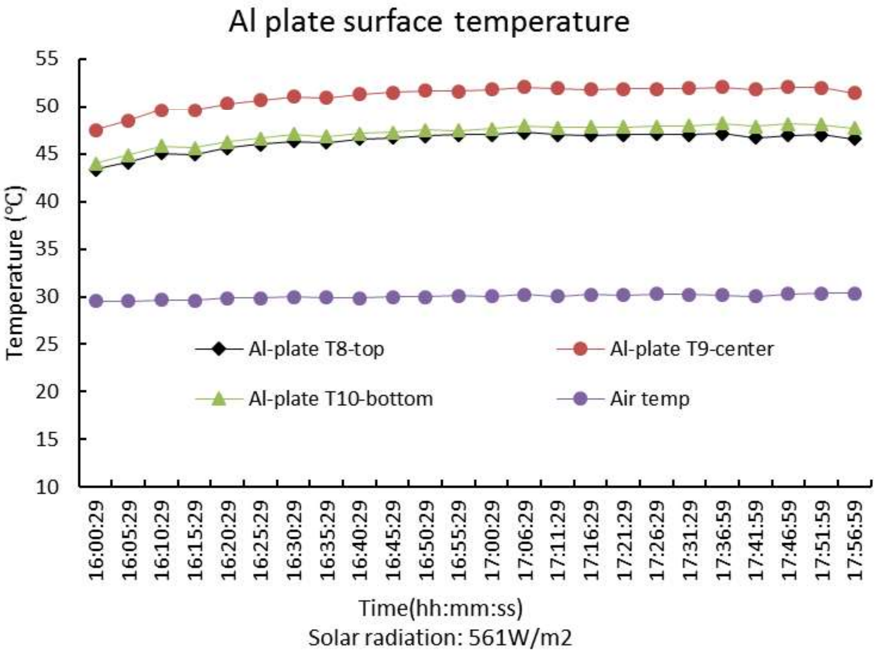

(b)

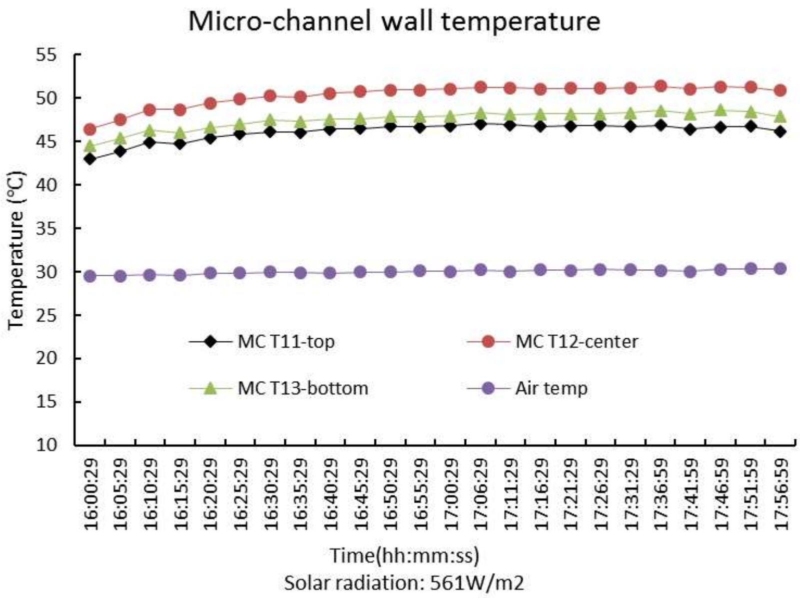

(c)

Figure 7. Temperature distribution of different components for the PV/T panel

In view of different layers of the panel, as shown in **Figure 8,** it is surprising to see that the aluminium plate in the mid-layer achieved a little higher temperature compared to the PV surface and micro-channel evaporator which were above and below the aluminium plate respectively. This indicates that the heat transfer across the panel was two-directional: one part of the heat is transferred from the aluminium plate to ambient and the other part is directed into the refrigerant within the LHP evaporator.

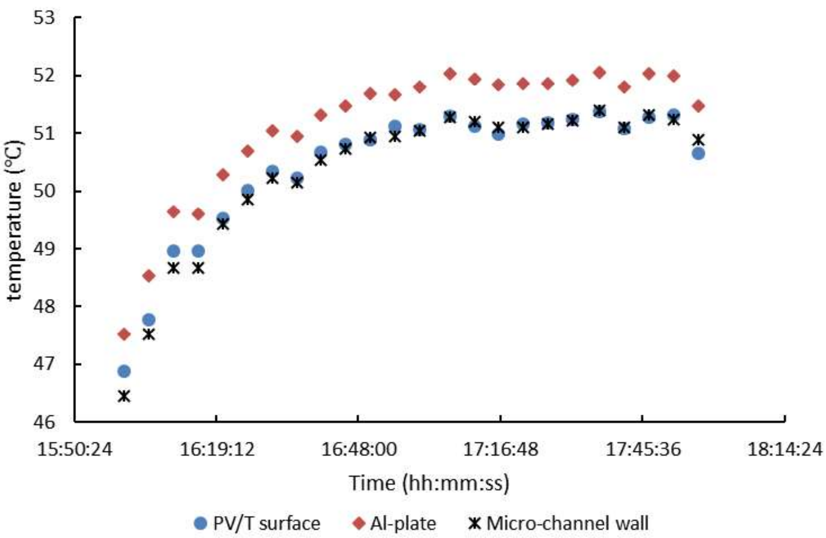

Figure 8. Temperature of different components of PV/T panel vs Operating time

5.3 Effect of different cooling water flow rate for optimal height difference under steady solar radiation

With the red points and the text figures showing the means of solar thermal efficiency of different flow rate groups, **Figure 9** shows variation of the solar thermal efficiency of the system against the cooling water flow rate. It is clear to see that the thermal efficiency of this vertical system increased obviously with the increase of the cooling water flow rate firstly and then lightly. This is due to the fact that as the cooling water flow rate is increasing, so the heat transfer rate between the refrigerant within the interior channel of the co-axial tubular exchanger and the cooling water within the mid-channel of the exchanger is rising. This led to higher heat transfer rate of the vertical MCLHP, reflected in increasing refrigerant flow rate. As a result, the heat loss of the vertical LHP-PV/T panel to ambient decreased and solar thermal efficiency of the system increased. With this specific operational condition, the average solar thermal efficiency of this vertical system raised from 42.79% to 50.85% while the cooling water flow rate increased from 0.05m3/h to 0.17 m3/h.

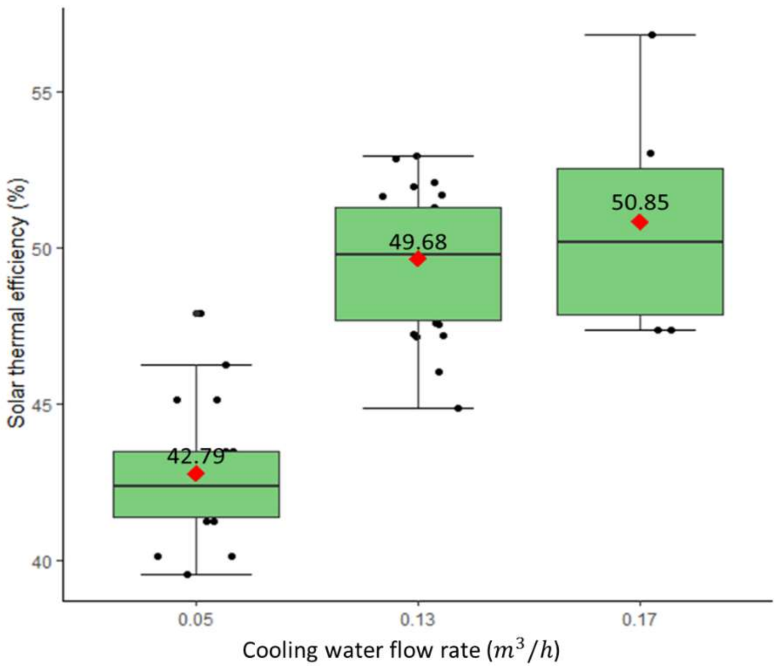

Figure 9. Solar thermal efficiency against cooling water flow rate

5.3 Effect of different air temperature for optimal height difference under steady solar radiation

The effect on solar thermal efficiency of different ambient air temperature was experimentally compared in groups and discussed. The results are shown in Figure 10 with the red points and the text figures showing the means of solar thermal efficiency of different groups. When keeping solar radiation at 560±5W/m2, cooling water flow rate at $0.17m^3/h$ at optimal height difference unchanged. The different ambient air temperature is corresponding to different solar thermal efficiency, which can be observed that with the increase of the air temperature from 24.1℃ to 30 ℃, the solar thermal efficiency has an obvious increase tendency from 46.72% to 57.48%. The reason for this phenomenon is that the increasing ambient air temperature would decrease the heat transfer performance between the PV/evaporator panel surface and the surrounding and thus the heat loss from the vertical LHP-PV/T panel surface to the ambient became less. Therefore, the average system solar thermal efficiency is improved.

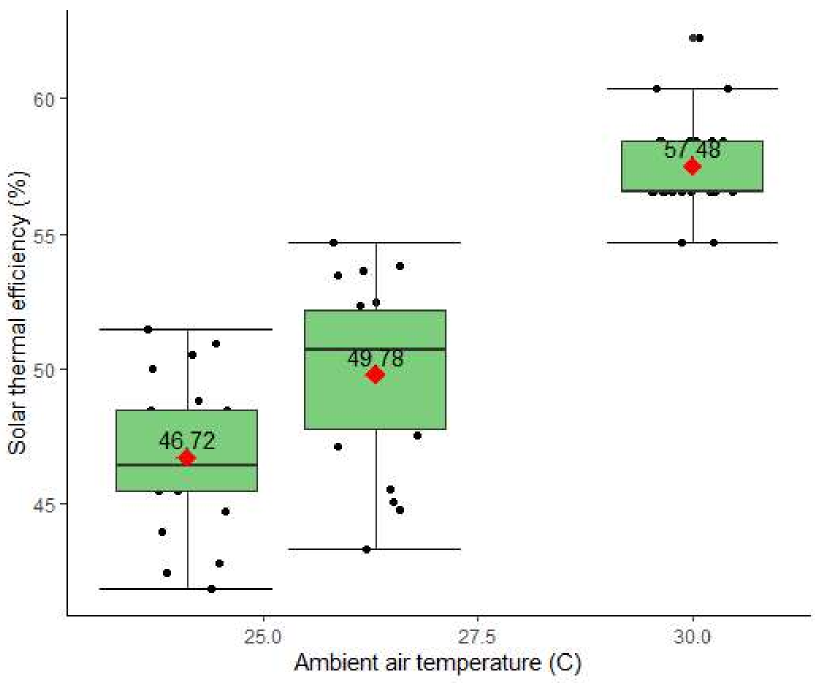

Figure 10. Solar thermal efficiency vs ambient air temperature.

5.3 Transient state response for optimal height difference under real weather

In this section, the transient solar thermal and electrical performance of this novel LHP-PV/T system with an optimal height difference of 1.1 m was investigated under real weather condition (experiment was carried out on 22nd Dec. 2018 in GDUT, China). **Figure 9** presents the PV module temperature, ambient air temperature and solar radiation under real weather during the outdoor testing day. The solar radiation was in the range of 250 to 610 W/m^2, and the ambient temperature is around 22 to 29 °C. It is found that the PV module temperature is sensitively changing with the solar radiation, and it is interesting to observe that the temperatures from bottom to top along the PV module surface were lower than 60 ℃ and were almost in equivalence at the same moment, respectively. This is owing to the fact that the solar radiation to different position of the PV module surface are uniform at the same time under the real weather, which is superior to the performance of this system.

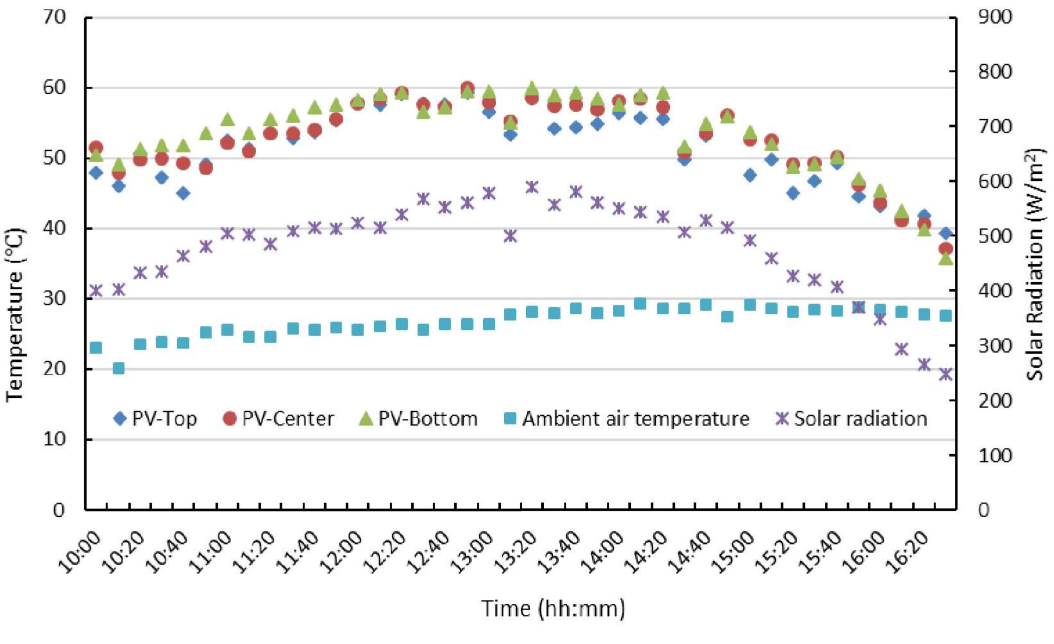

Figure 9 PV module temperature, ambient air temperature and solar radiation under real weather

The transient solar thermal and electrical performance of this novel LHP-PV/T system with an optimal height difference of 1.1 m are illustrated in **Figure 10.** Under these specific operational conditions and the real weather solar radiation, the solar thermal efficiency of the system was in the range from 34.8% to 71.4%, the solar electrical efficiency was in range from 9.2% to 18.8%, and overall efficiency was in range from 51.2% to 88.4% respectively, which are higher than most of existing conventional solar heat pipe PV/T system. It is obvious that the solar thermal efficiency is not sensitive to the solar radiation, where there is always lagging response and even opposite trend, reflecting that the transient heat transfer process is not sensitive to the solar radiation; and the solar electrical efficiency almost keeps the same value during the testing time and has the opposite trend with the PV module temperature, which complied well with the common knowledge of the solar PV/T system that PV panels normally have linear drop-off in efficiency as the surface temperature rises, which typically lose efficiency of up to 0.4% per degree centigrade rise in the PV-cells' temperature (Luque et al., 2003; Chow, 2010).

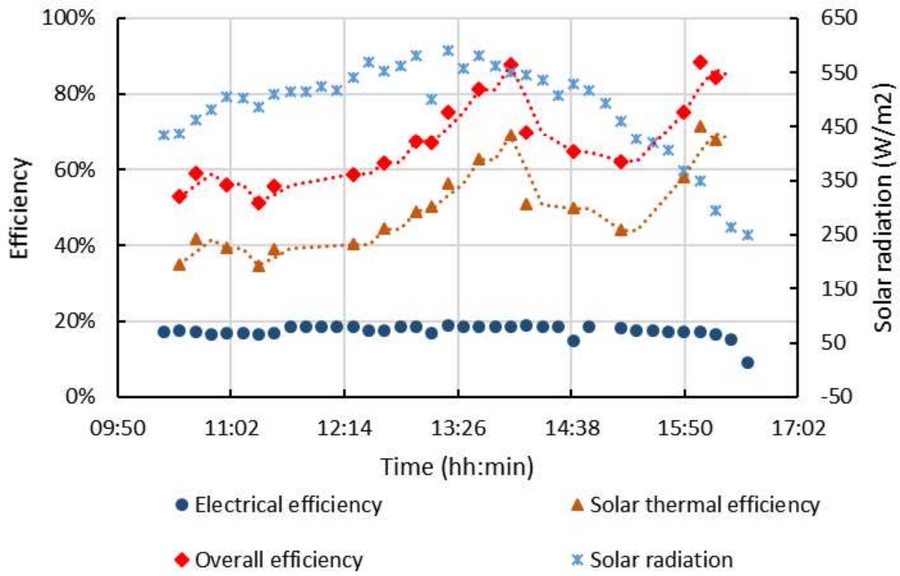

Figure 10. Solar thermal and electrical performance under real weather

6 Conclusion

In this paper, the impact of the height difference (HD) between the evaporator and the condenser on the solar thermal performance of the novel LHP-PV/T system was experimentally investigated. Various tests were carried out to find out the optimal value of the height difference between the PV/evaporator and the condenser to optimize the system construction and thus helping to develop a high thermal performance and low-cost solar PV/T system for domestic use. The conclusions were summarized as follows:

(1) Under the specific operational and testing condition, the parabola-like trend of the solar thermal efficiency variation with the different height difference is obvious, where the maximum thermal efficiencies takes place at the height difference of 1.1m, which is considered as the optimal value of height difference between heat exchanger and evaporator. In addition the height difference of 1.1 m can make the system more compact leading to a lower cost than that of 1.3m.

(2) When the system operates at the steady state condition, the PV module surface temperature is decreased with the increase of the height difference.

(3) The aluminium plate in the mid-layer achieved a little higher temperature compared to the PV surface and micro-channel evaporator which were above and below the aluminium plate respectively, indicating that the heat transfer across the panel was two-directional.

(4) Under the specific operational conditions and the real weather solar radiation, the solar thermal efficiency of the system was in the range of 34.8% to 71.4%, the solar electrical efficiency was in range of 9.2% to 18.8%, and overall efficiency was in range of 51.2% to 88.4% respectively, which are higher than most of the existing conventional solar heat pipe PV/T system. In addition, the solar thermal efficiency is not sensitive to the solar radiation, where there is always lagging response and even opposite trend. This indicated that the transient heat transfer process is not sensitive to the solar radiation.

Acknowledgements: The authors would acknowledge our appreciation to the financial supports from the EPSRC (EP/R004684/1) and Innovate-UK (TSB 70507-481546) for the Newton Fund – China-UK Research and Innovation Bridges Competition 2016 Project 'A High Efficiency, Low Cost and Building Integrate-able Solar Photovoltaic/Thermal (PV/T) System for Space Heating, Hot Water and Power Supply', from the UK BEIS for the project titled 'A low carbon heating system for existing public buildings employing a highly innovative multiple-throughout-flowing micro-channel solar-panels-array and a novel mixed indoor/outdoor air source heat pump', from Department of Science and Technology of Guangdong Province, China (2018A050501002 & 2019A050509008), European Commission H2020-MSCA-RISE-2016 Programme (734340-DEW-COOL-4-CDC), European Commission

H2020-MSCA-IF-2018 Programme (835778-LHP-C-H-PLATE-4-DC), and Dongguan Innovative Research Team Program (No. 2014607101008). Furthermore, the authors would also acknowledge the financial support from Chinese Scholarship Council for a UoH-CSC PhD programme.

Reference

[1] International Energy Agency (IEA). Market Report Series Renewables 2O18 Analysis and Forecast to 2023. 2018.

[2] Luque A, Hegedus S. Handbook of Photovoltaic Science and Engineering. 2003. https://doi.org/10.1002/0470014008.

[3] Skoplaki E, Palyvos JA. On the temperature dependence of photovoltaic module electrical performance: A review of efficiency/power correlations. Solar Energy 2009;83:614–24. https://doi.org/https://doi.org/10.1016/j.solener.2008.10.008.

[4] Chow TT. A review on photovoltaic/thermal hybrid solar technology. Applied Energy 2010;87:365–79. https://doi.org/10.1016/j.apenergy.2009.06.037.

[5] Zhou J, Zhao X, Yuan Y, Li J, Yu M, Fan Y. Operational performance of a novel heat pump coupled with mini-channel PV/T and thermal panel in low solar radiation. Energy and Built Environment 2020;1:50–9. https://doi.org/https://doi.org/10.1016/j.enbenv.2019.08.001.

[6] Hussain F, Othman MYH, Sopian K, Yatim B, Ruslan H, Othman H. Design development and performance evaluation of photovoltaic/thermal (PV/T) air base solar collector. Renewable and Sustainable Energy Reviews 2013;25:431–41. https://doi.org/https://doi.org/10.1016/j.rser.2013.04.014.

[7] Delisle V, Kummert M. A novel approach to compare building-integrated photovoltaics/thermal air collectors to side-by-side PV modules and solar thermal collectors. Solar Energy 2014;100:50–65. https://doi.org/https://doi.org/10.1016/j.solener.2013.09.040.

[8] Fraisse G, Ménézo C, Johannes K. Energy performance of water hybrid PV/T

collectors applied to combisystems of Direct Solar Floor type. Solar Energy 2007;81:1426–38. https://doi.org/https://doi.org/10.1016/j.solener.2006.11.017.

[9] Herrando M, Markides CN, Hellgardt K. A UK-based assessment of hybrid PV and solar-thermal systems for domestic heating and power: System performance. Applied Energy 2014;122:288–309. https://doi.org/https://doi.org/10.1016/j.apenergy.2014.01.061.

[10] Long H, Chow TT, Ji J. Building-integrated heat pipe photovoltaic/thermal system for use in Hong Kong. Solar Energy 2017;155:1084–91. https://doi.org/10.1016/j.solener.2017.07.055.

[11] Zhang X, Zhao X, Xu J, Yu X. Characterization of a solar photovoltaic/loop-heat-pipe heat pump water heating system. Applied Energy 2013;102:1229–45. https://doi.org/https://doi.org/10.1016/j.apenergy.2012.06.039.

[12] Zhang X, Zhao X, Shen J, Xu J, Yu X. Dynamic performance of a novel solar photovoltaic/loop-heat-pipe heat pump system. Applied Energy 2014;114:335–52. https://doi.org/10.1016/j.apenergy.2013.09.063.

[13] He W, Hong X, Zhao X, Zhang X, Shen J, Ji J. Operational performance of a novel heat pump assisted solar façade loop-heat-pipe water heating system. Applied Energy 2015;146:371–82. https://doi.org/10.1016/j.apenergy.2015.01.096.

[14] Reay DA, Kew PA, McGlen RJ. Chapter 6 - Special types of heat pipe. In: Reay DA, Kew PA, McGlen RJ, editors. Heat Pipes (Sixth Edition). Sixth Edit, Oxford: Butterworth-Heinemann; 2014, p. 135–73. https://doi.org/https://doi.org/10.1016/B978-0-08-098266-3.00006-6.

[15] Yu M, Diallo TMO, Zhao X, Zhou J, Du Z, Ji J, et al. Analytical study of impact of the wick’s fractal parameters on the heat transfer capacity of a novel micro-channel loop heat pipe. Energy 2018;158:746–59. https://doi.org/10.1016/j.energy.2018.06.075.

[16] Diallo TMO, Yu M, Zhou J, Zhao X, Shittu S, Li G, et al. Energy performance analysis of a novel solar PVT loop heat pipe employing a microchannel heat

pipe evaporator and a PCM triple heat exchanger. Energy 2019;167. https://doi.org/10.1016/j.energy.2018.10.192.

[17] Ling L, Zhang Q, Yu Y, Liao S, Sha Z. Experimental study on the thermal characteristics of micro channel separate heat pipe respect to different filling ratio. Applied Thermal Engineering 2016;102:375–82. https://doi.org/10.1016/j.applthermaleng.2016.03.016.

[18] Diallo TMO, Yu M, Zhou J, Zhao X, Ji J, Hardy D. Analytical investigation of the heat-transfer limits of a novel solar loop-heat pipe employing a mini-channel evaporator. Energies 2018;11. https://doi.org/10.3390/en11010148.

[19] Zhao X, Wang Z, Tang Q. Theoretical investigation of the performance of a novel loop heat pipe solar water heating system for use in Beijing, China. Applied Thermal Engineering 2010;30:2526–36.

[20] Zhang X, Shen J, Adkins D, Yang T, Tang L, Zhao X, et al. The early design stage for building renovation with a novel loop-heat-pipe based solar thermal facade (LHP-STF) heat pump water heating system: Techno-economic analysis in three European climates. Energy Conversion and Management 2015;106:964–86. https://doi.org/10.1016/j.enconman.2015.10.034.

[21] Zhang X. Investigation of a Novel Solar Photovoltaic/Loop-Heat-Pipe Heat Pump System. University of Hull, 2014. https://hydra.hull.ac.uk/resources/hull:8422.

[22] Ren X, Yu M, Zhao X, Li J, Zheng S, Chen F, et al. Assessment of the cost reduction potential of a novel loop-heat-pipe solar photovoltaic/thermal system by employing the distributed parameter model. Energy 2020;190:116338. https://doi.org/10.1016/j.energy.2019.116338.

[23] Su Q, Chang S, Yang C. Loop heat pipe-based solar thermal façade water heating system: A review of performance evaluation and enhancement. Solar Energy 2021;226:319–47. https://doi.org/10.1016/j.solener.2021.08.019.

[24] Li G, Pei G, Ji J, Yang M, Su Y, Xu N. Numerical and experimental study on a PV/T system with static miniature solar concentrator. Solar Energy

2015;120:565–74. https://doi.org/https://doi.org/10.1016/j.solener.2015.07.046.

[25] Li G, Diallo TMO, Akhlaghi YG, Shittu S, Zhao X, Ma X, et al. Simulation and experiment on thermal performance of a micro-channel heat pipe under different evaporator temperatures and tilt angles. Energy 2019;179:549–57. https://doi.org/https://doi.org/10.1016/j.energy.2019.05.040.

[26] Diallo TMO, Yu M, Zhou J, Zhao X, Shittu S, Li G, et al. Energy performance analysis of a novel solar PVT loop heat pipe employing a microchannel heat pipe evaporator and a PCM triple heat exchanger. Energy 2019;167:866–88. https://doi.org/10.1016/j.energy.2018.10.192.

[27] Yu M, Chen F, Zheng S, Zhou J, Zhao X, Wang Z, et al. Experimental Investigation of a Novel Solar Micro-Channel Loop-Heat-Pipe Photovoltaic/Thermal (MC-LHP-PV/T) System for Heat and Power Generation. Applied Energy 2019;256:113929. https://doi.org/10.1016/j.apenergy.2019.113929.

[28] Zhang X, Zhao X, Xu J, Yu X. Characterization of a solar photovoltaic/loop-heat-pipe heat pump water heating system. Applied Energy 2013;102:1229–45. https://doi.org/10.1016/j.apenergy.2012.06.039.

[29] Chen CQ, Diao YH, Zhao YH, Wang ZY, Zhu TT, Wang TY, et al. Numerical evaluation of the thermal performance of different types of double glazing flat-plate solar air collectors. Energy 2021;233:121087. https://doi.org/https://doi.org/10.1016/j.energy.2021.121087.

[30] Swamee PK, Swamee N. Discharge equation of a circular sharp-crested orifice. Journal of Hydraulic Research 2010;48:106–7.

[31] Shabanlou, Saeid. Improvement of Extreme Learning Machine Using Self-Adaptive Evolutionary Algorithm for Estimating Discharge Capacity of Sharp-Crested Weirs Located on the end of Circular Channels. Flow Measurement and Instrumentation 2017:S0955598617301942.